Smart Microcapsules from Porphyrin-nanogold Hybrids towards light-triggered release

Tiago José de Ceia Charana

November 2021

Integrated Master's student in Chemical Engineering at Instituto Superior Técnico, Universidade de Lisboa, Lisbon, Portugal

ABSTRACT: The aim of this work is the development of a photoactive polyelectrolyte microcapsule system with improved optical and structural properties that enables its application in drug delivery systems, bioimaging and photodynamic therapy of tumor tissues. The hybrid systems were constituted by a porphyrin photosensitizer, TMPyP (5,10,15,20-tetrakis(4-N-methylpyridinium) porphyrin and gold nanorods that promotes fluorescence increase of the photosensitizer through plasmonic effects.

The characterization of the optical, photodynamic and structural properties of the systems was followed by UV-Vis absorption spectroscopy and scanning electron microscopy (SEM). The main target in the study of these systems is related with fluorescence intensification caused by modifications in relative position of gold nanorods and porphyrin. The adsorption of oppositely charged polyelectrolytes was followed by zeta potential measurements. Using FLIM technique, the values of the fluorescence intensification events were about 10^4 and 10^5.

The production of singlet oxygen was studied by UV-Vis spectroscopy based on 1,3-diphenylisobenzofuran (DPBF) degradation. Singlet oxygen formation was the result of the irradiation of the systems containing porphyrin in the core or in the shell and we can say that the amount of singlet oxygen formed is greater in the latter.

Two cytotoxicity assays were carried out using HeLa cells. In one of the assays, the plate containing the compounds studied before was irradiated. Resazurin was used as an indicator of cell viability, and it can be inferred that cell death is more effective in the irradiated plate.

KEYWORDS: Microcapsules, Porphyrin, Polyelectrolytes, Gold Nanorods, Singlet Oxygen, Cytotoxicity.

INTRODUCTION

According to World Health Organization, in 2019 cancer was one of the leading causes of death worldwide, ranking ahead of other diseases, such as stroke and coronary heart disease. In 2020, around 19.3 million new cases of cancer were registered, resulting in the death of 10 million people [1].

Current diagnostic methods, such as X-ray, mammography, Magnetic Resonance Imaging (MRI) and computed tomography (CT), are time-consuming, expensive and complex [2].

The most common treatment methods have several limitations and drawbacks that need to be overcome, such as clinical dose, selectivity, pain, hair loss and chemoresistance [3]. Thus, it is necessary to develop new systems that can act as detection and therapeutic agents.

Photodynamic therapy (PDT) is in a prime position on this field because it can be used in inoperable tumors and to treat early or localized tumors in a selective and effective way, with less secondary effects and without compromising adjacent healthy tissues [4]. Plus, PDT presents good results even when combined with traditional techniques [5] and it involves a photosensitizer (PS) which is a molecule responsible for the production of Singlet Oxygen ($^1O_2$) capable of inducing tumor cell death. Ideally, a PS should be a pure, stable and non-toxic compound with tendency to accumulate in tumor cells as well as a long-lived triplet excited state. Besides, it should be easy to store and activation must be done with a wavelength appropriate for tissue penetration[6][7].

After light absorption, PS migrates from fundamental state to a singlet excited state, from which it can decay directly back to fundamental state by fluorescence emission.

On the other hand, can occur an electronic spin conversion to a triplet excited state [7]. The energy transfer from PS depends on oxygen availability in tumor tissue. For low O_2 concentration, PS reacts with other organic molecules available in the substrate generating Reactive Oxygen Species (ROS). For high O_2 concentrations, PS directly transfer its energy to molecular oxygen resulting in singlet oxygen formation ($^1O_2$), which is a very cytotoxic species for cancer cells [7][8].

Porphyrins are a class of compounds highly available in nature, biocompatible and non-toxic with the capacity of selectively accumulate in tumoral tissues, so that, many porphyrins are used as photosensitizers. Moreover, porphyrins can generate oxygen species highly reactive and after activation by light, porphyrins emit fluorescence and therefore they can be used as contrast agent for bioimaging detection [6][7].

However, a large part of the porphyrins are weak emitters, and their fluorescence can be improved conjugating them with metallic nanoparticles [9]. In this work we use Gold Nanoparticles (GNPs) to increase porphyrin fluorescence. GNPs are easily synthetized, biocompatible and resistant to photochemical degradation [10]. These particles exhibit an optical property called Localized Surface Plasmon Resonance (LSPR) which consists in a collective and coherent oscillation of the electrons confined by the surface of the nanoparticle, under radiation [10][11]. The LSPR excitation of the nanoparticles generates strong confined electromagnetic fields, which increase the probability of light absorption by a fluorophore that is in the vicinity and, consequently, also increases the number of photons emitted by fluorescence [11].

To combine these two components (porphyrin and GNPs), promoting a fluorescence enhancement and the transport, storage and delivery of biologic compounds in living organisms it was decided to build polyelectrolyte microcapsules. Polyelectrolyte capsules were constructed using a layer-by-layer method, in which oppositely charged polyelectrolytes are adsorbed on a particle mold due to electrostatic interactions [12].

There are many other examples of compounds that can transport and deliver biological material, such as: liposomes and fullerenes [13]. However, polyelectrolyte microcapsules stand out compared to other delivery systems because they can be functionalized with a variety of molecular compounds, present a great load capacity and their synthesis does not require extreme experimental conditions, neither the use of extremely expensive technological devices [12].

In this dissertation is shown the development of a porphyrin-gold hybrid, constituted by a tetracationic porphyrin 5,10,15,20-tetrakis (N-metil-4-pyridynium) [TMPyP] and gold nanorods (AuNR), located in polyelectrolytes microcapsules with a polystyrene core and coated with two different polyelectrolytes (PSS and PAH).

EXPERIMENTAL SECTION

Materials: Poly styrenesulfonate [PSS (MM≈75000 g/mol, 18% %m/v)] (MM≈75000 g/mol, 18% %m/v)] and Polyallylamine hydrochloride, [PAH (MM≈50000 g/mol) ou (MM≈17500 g/mol)] were obtained from Sigma Aldrich. Sodium chloride [NaCl (MM≈58.44 g/mol, >=99,5%)] was purchased from Fisher Chemical. Polystyrene microparticles [PS, 1.04 µm, SD=0.035 µm, 10% w/v, d=1.05 g/cm^3] were purchased in microparticles GmbH Forschungs- und Entwicklungslaboratorium. Sodium carbonate [Na_2CO_3 (MM≈105.99 g/mol)] and calcium chloride [$CaCl_2$ (MM≈147.02 g/mol)] were obtained from J. T. Baker and Merck, respectively. Sodium hydroxide [NaOH (MM≈40.00 g/mol)] and hydrochloric acid [HCl (7%)] were purchased from Sigma Aldrich, for pH adjustments. 5,10,15,20-Tetrakis(4-N-methylpyridinium)porphyrin [TMPyP (MM~1363.6 g/mol)] was obtained from Sigma Chemicals. Gold nanorods, coated with CTAB, with an approximate size of 25 nm × 71 nm were acquired from Nanopartz Inc. as aqueous suspensions with an optical density of 1 (product no. A12-25-650-CTAB-DIH-1-25, batch 12G72-10253 with λ_{LSPR}=659 nm, λ_{TSPR}=516 nm and product no. A12-25-600-CTAB-DIH-1-25, batch 12G70-10253 with λ_{LSPR}=614 nm, λ_{TSPR}=523 nm). Resazurin solution (0.1 mg/mL) and 10% FBS DMEM solution.

Preparation of $CaCO_3$ and PS microparticles: For $CaCO_3$ microcapsules a $CaCl_2$ solution (0.33 M) was added to an equal volume of a Na_2CO_3 (0.33 M) with PSS (4 g/L)

solution. This mixture was mixed for 30 seconds under intense stirring and let to rest for 15 minutes. $CaCO_3$ cores free of non-adsorbed reagents were recovered after 3 centrifugation/washing cycles with distilled H_2O (3000 rpm, 5 minutes). Then, microparticles were dispersed in a polyelectrolyte aqueous solution of PSS (1 mL, C_{PSS}=3 mg/mL, 0.5 M NaCl, pH 6.5) and PAH (1 mL, C_{PAH}=3 mg/mL, 0.5 M NaCl, pH 6.5). After intense stirring (15 minutes for PSS and 1h for PAH) and a centrifugation cycle (3000 rpm, 5 minutes), the supernatant was removed, and polyelectrolyte microcapsules recovered. To remove the excess of polyelectrolyte, three centrifugation/washing cycles were performed (3000 rpm, 5 minutes) after each adsorption. Between each step of centrifugation, the sample was subjected to ultrasounds and vortex agitation.

For PS microcapsules, 50 µL of commercial polystyrene microparticles ($8.09x10^9$ particles) were dispersed in a aqueous PAH solution (5 mL, C_{PAH}=3 mg/mL, 0.5 M NaCl, pH=6.5). After 1h of intense stirring. Then, the system was again dispersed in an aqueous PSS solution (10 mL, C_{PSS}=3 mg/mL, 0.5 M NaCl, pH=6.5) during 15 minutes under intense stirring. To remove the excess of polyelectrolyte, three centrifugation/washing cycles were performed (3000 rpm, 5 minutes) after each adsorption step. The number of polyelectrolytes (PSS/PAH) layers adsorbed by layer-by-layer technique depends on the system architecture and the charge of each layer was measured by Zeta Potential.

Porphyrin incorporation onto microparticles: TMPyP ($2.3x10^{-5}$ M) was incorporated in microparticles by a co precipitation reaction while $CaCO_3$ cores are formed. The volume of TMPyP solution added is 2 times less than the volumes of the Na_2CO_3 and $CaCl_2$ solutions. After intense stirring (30 seconds) and resting (15 minutes), three centrifugation/washing cycles (3000 rpm, 5 minutes) with distilled H_2O were performed, to recover microparticles free of non-adsorbed reagents.

For PS microcapsules, TMPyP was adsorbed onto a PSS layer ($4.6x10^{-6}$ M), under intense stirring (1 hour), followed by two centrifugation cycles (6000 rpm, 10 minutes) to obtain functionalized microparticles free of non-adsorbed porphyrin.

Gold nanorods incorporation onto microparticles: First, gold nanorods were centrifuged (6000 rpm, 15 minutes) to remove the CTAB excess. Then, AuNR were dispersed in a solution of PSS (1 mL, C=1.7 mg/mL, 1 mM NaCl) through intense stirring (1 h) followed by three centrifugation/washing cycles (5000 rpm, 10 minutes) to achieve non-adsorbed reagent free microparticles. After that, functionalized AuNR were adsorbed onto PAH layer of the polystryrene microcapsules. $2.5x10^{10}$ particles of AuNR were added to a solution of microcapsules containing $4.045x10^9$ particles through intense stirring (1h) followed by one centrifugation/washing cycle (6000 rpm, 10 minutes).

Methods: A Lambda 35 spectrophotometer from PerkinElmer was used in UV-Vis absorption measurements.

Fluorescence emission was recorded with a Fluorolog FL-1040 spectrofluorimeter from Horiba Jobin Yvon.

pH adjustments were performed in Denver Instrument Model 15 sensor and Mettler Toledo AG 30281915 Rev A electrode, at 25ºC.

Zeta potential values were measured in a Doppler electrophoretic light scattering analyzer Zetasizer Nano ZS from Malvern Instruments Ltd.

Scanning Electron Microscopy (SEM) images were obtained by Hitachi S2400 microscope (25kV).

FLIM measurements were performed with a time-resolved confocal microscope, MicroTime 200 from PicoQuant GmbH. The excitation energy at 639 nm was provided by pulsed diode laser at a repetition rate of 20 MHz. The fluorescence lifetime was detected with a single-photon counting avalanche diode (SPAD) from PerkinElmer, whose signal was processed by TimeHarp 200 TC-SPC PSboard from PicoQuant working in a time-tagged time resolved (TTTR) operation mode. The Olympus IX 71 inverted microscope coupled with a water immersion objective allowed an optical analysis.

RESULTS AND DISCUSSION

In this section is shown the development of photoactive hybrids of polyelectrolyte microcapsules containing TMPyP and AuNR

with the objective of increasing the fluorescence of the system, enabling its application in bioimaging/photodynamic therapy of cancer cells.

According with previous studies, to achieve fluorescent enhancement of a molecule near a nanometallic particle it requires the overlap of the absorption and emission spectra of the fluorophore with the resonance plasmon of the metallic nanoparticle [14].

TMPyP absorption spectrum in water exhibits several bands in the visible region of the electromagnetic spectrum: the Soret band (λ≈420 nm) and four Q bands (λ≈500-700 nm). Its emission spectrum occurs at λ≈600-800 nm. Gold nanorods absorb at λ≈520 and λ≈660 nm, that corresponds to its transversal and longitudinal plasmons [15].

Once demonstrated the TMPyP-AuNR overlap, these two components can interact with each other and so that the possibility of TMPyP fluorescence intensification due to nanorods justifies the hybrid system proposed in this work.

Figure 1 presents the structures of all the systems studied in this work.

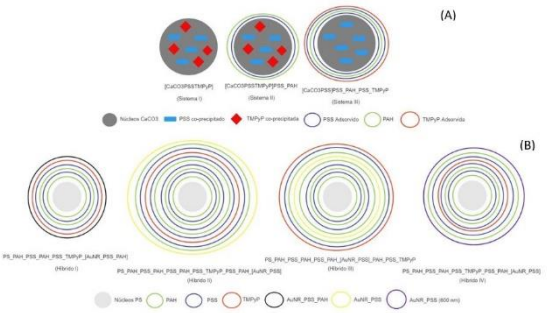

Figure 1 - Schematic Representation of the Architectures of the Studied Systems constituted by $CaCO_3$ (A) or PS (B) cores.

The hybrids studied throughout this dissertation require an in-depth study of the adsorption efficiency of each of the components, as well as the photophysical, spectroscopic, morphological and biological properties of the constituents individually and together in a system. Therefore, the optimization of experimental conditions for the design of these systems was a very important and time-consuming part of this work. In order to relate the architectures of the systems with the possible photodynamic effect, it was also carried out the study of singlet oxygen production by the systems I, II and III.

Polyelectrolyte Microcapsules with calcium carbonate cores (CaCO3) and coated with Polyelectrolytes (PSS and PAH):

$CaCO_3$ microparticles were prepared through a precipitation reaction of calcium chloride ($CaCl_2$) and sodium carbonate (Na_2CO_3) [16].

First, $CaCO_3$ microparticles were dispersed in a PSS solution ((MM = 75000 g/mol), 3 mg/mL, 0.5 M NaCl e pH=6.5) and then in a PAH solution ((MM = 17500 g/mol), 13 mg/mL, 0.5M NaCl e pH=6.5). Under these experimental conditions, the adsorption of the polyelectrolyte layers was successful since, after the first adsorption of the negatively charged polyelectrolyte (PSS), the value of the zeta potential was about -40 mV, while at the end of the adsorption of the positively charged polyelectrolyte (PAH) the charge of the surface was completely reversed (ξ= +38 mV).

However, FLIM images show that after adsorption of PAH there is an increase in fluorescence of the microcapsules caused by a impurity present in PAH (Figure 2-(B)).

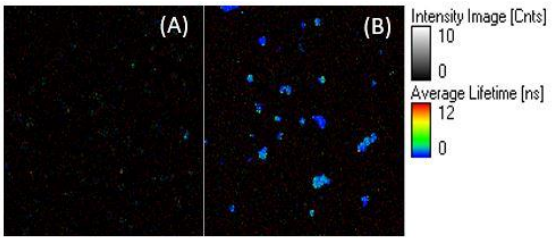

Figure 2 - FLIM images (80x80 μm) comparing the fluorescence of $CaCO_3$ cores (A) with cores coated with a polyelectrolyte bilayer (PSS_PAH) (B) (λ_{exc} = 635 nm, I = 1000 a.u.).

Therefore, the protocol described above was repeated but using PAH with a higher molecular weight (MM = 50 000 g/mol) and lower concentration (3 mg/mL). In these conditions, we obtained some spherical microparticles and aggregates too.

Indirect measurement of singlet oxygen production by TMPyP

For systems I and II, TMPyP was incorporated in microparticles by a co precipitation reaction at the same time that $CaCO_3$ cores were formed (System I – C_{TMPyP} = 3 μM; System II – C_{TMPyP} = 0.08 μM). For System II, $CaCO_3$ microparticles were coated with a bilayer of polyelectrolytes (PSS/PAH). In the case of system III, there is no porphyrin in the core and TMPyP was adsorbed over a PSS layer (System III – C_{TMPyP}

= 1.2 μM) and the microcapsules were recovered after 3 centrifugation/washing cycles (3000 rpm, 5 min).

Irradiation promotes the production of singlet oxygen by TMPyP which was evaluated through 1,3-diphenylisobenzofuran (DPBF) oxidation in DMF (Figure 3).

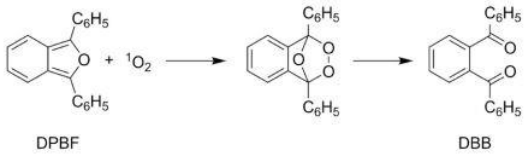

Figure 3 - Cycloaddition reaction undergone by DPBF in the presence of Singlet oxygen ($^1O_2$) [17].

In all the assays DPBF concentration was kept constant (25 μM), as well as the irradiation power (≈6.50 mW/cm^2). DPBF is a photosensitive compound that absorbs at λ = 416 nm. Consequently, it was used a cut-off filter which guarantees that only radiation with a wavelength greater than 550 nm reaches the sample, ensuring that the degradation of DPBF is only due to the reaction with singlet oxygen generated by the photosensitizer (TMPyP).

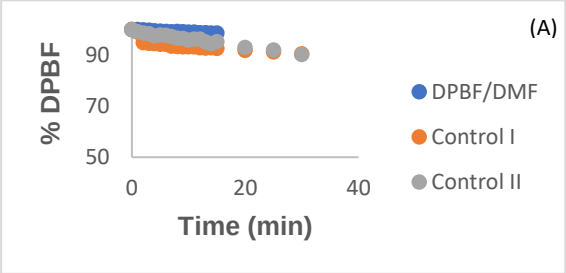

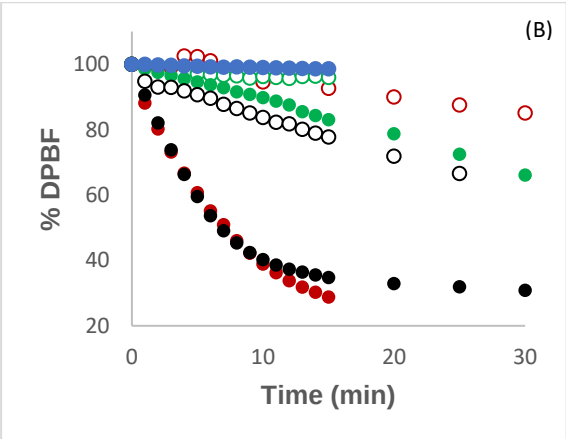

Figure 4 – DPBF oxidation in all the controls (A) and systems containing porphyrin (B). System I - 3 μM (—), System II – 0,08 μM (—) and System III – 1,2 μM(—).

According to Figure 4-(A), there is no DPBF oxidation in control systems (without porphyrin). In Figure 4-(B), solutions of TMPyP were prepared with the same concentration as the systems containing porphyrin (System I – C_{TMPyP}= 3 μM; System II – C_{TMPyP}= 0.08 μM; System III – C_{TMPyP}= 1.2 μM). For the system with porphyrin adsorbed in the shell, DPBF degradation was about 34% while for systems I and II containing porphyrin on the core, that degradation was only about 15%. In conclusion, it can be said that systems with porphyrin located inside the core are not effective in the production of singlet oxygen and, as such, the adsorption of the photosensitizer on the microcapsule surface layer is more favourable for this purpose.

TMPyP photostability

To evaluate the photostability of porphyrin, emission spectra of TMPyP in DMF+DPBF were plotted for the excitation wavelengths of 600 nm and 440 nm.

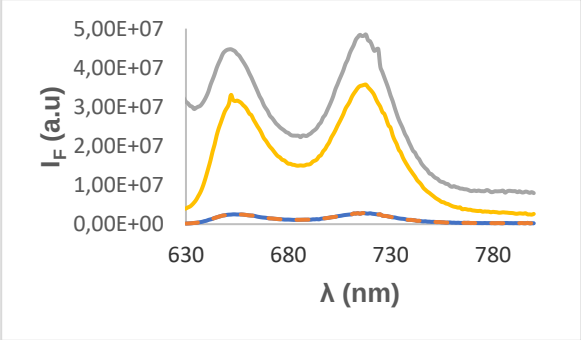

Figure 5 – Emission spectra of TMPyP (3 μM) in DMF before (—) and after (—) irradiation at λ_{exc}= 600 nm and before (—) and after (—) irradiation at λ_{exc}= 440 nm

The excitation wavelength of 600 nm corresponds to the region of the Q-bands of porphyrin. It can be seen the overlap, before and after irradiation, of the emission spectra of the TMPyP in DMF, which proves that porphyrin is photostable at this wavelength.

The UV-VIS absorption spectrum of DPBF in DMF shows an absorption band around λ = 420 nm and this compound in DMF emits fluorescence in λ close to 630 nm [18]. Hence, the intensity of the signal in the spectrum before irradiating is a result of the emission from porphyrin and DPBF. After irradiation, the

intensity of the signal obtained is lower because the DPBF has already been degraded by the singlet oxygen produced by TMPyP and, therefore, the intensity of the emission registered is only due to the porphyrin, which proves its photostability.

Polyelectrolyte Microcapsules PS cores and coated with Polyelectrolytes (PSS and PAH): To overcome the instability of the previously prepared systems, it was decided to replace the $CaCO_3$ cores by commercial polystyrene cores, which are more stable under our experimental conditions.

The procedure for the construction of polyelectrolyte microcapsules is described above and the surface charge after each adsortion of polyelectrolytes was measured by zeta potential (Figure 6).

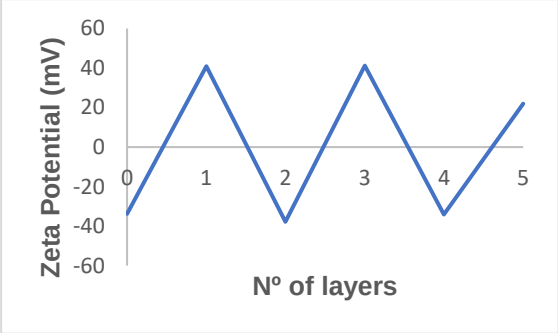

Figure 6 – Variation of Zeta Potential (ξ) of the system as a function of the number of adsorbed PAH and PSS layers.

It should be noted that the zeta potential value obtained for the polystyrene cores is -33.8 mV, so the PAH positive polyelectrolyte was first adsorbed.

Preparation of the system Hybrid I:
The hybrid system I resulted from the simultaneous mix of polystyrene cores coated by a double layer of PAH_PSS ($4.60x10^9$ particles) with a solution of TMPyP with a concentration equal to 2.3 μM and AuNR ($1x10^{11}$ particles) previously coated by a layer PSS and another from PAH.

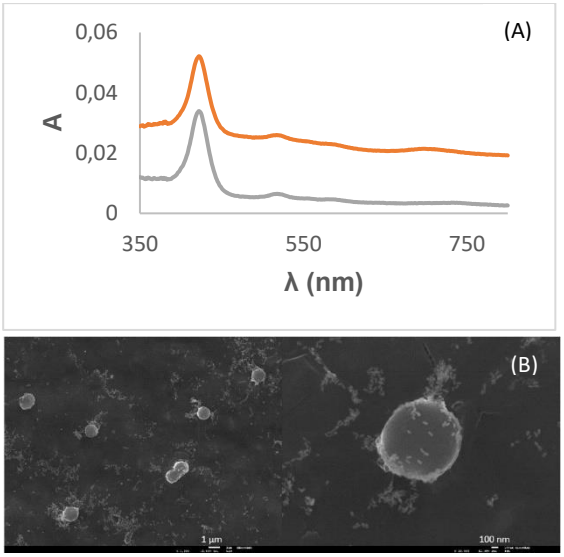

Figure 7 – UV-Vis absorption spectrum of hybrid system I (—) and supernatant (—) after adsorption of TMPyP and AuNR (A) and scanning electron microscopy image of hybrid I (B).

Absorbance of the supernatant solutions was measured to calculate the efficiency/adsorption capacity (EA) of this system through equation (1), as well as the number of moles of adsorbed porphyrin

$$EA = \frac{n_{ads}}{n_{ini}} \, x \, 100 \qquad (1)$$

Where n_{ads} corresponds to the number of moles adsorbed and n_{ini} corresponds to the number of moles of porphyrin in the adsorption solution.

Based on the data in figure 7-(A), the values obtained for the number of moles adsorbed and adsorption efficiency were $4.69x10^{-10}$ mol and 40.7%, respectively. SEM images (Figure 7-(B)) reveals micrometric structures weakly coated with gold nanoparticles and non-adsorbed gold nanoparticles strongly aggregated in the areas surrounding the microcapsules.

To avoid the large amount of gold nanoparticles that aggregate and do not adsorb to the microcapsules, for the other systems gold nanorods were only coated with a PSS layer.

Preparation of the systems Hybrids II and III:
In this system, TMPyP (4.6 μM) was incorporated through a self-assembly mechanism in which the pyridinium groups adsorb to the PSS negative layer of the microcapsules through electrostatic interactions.

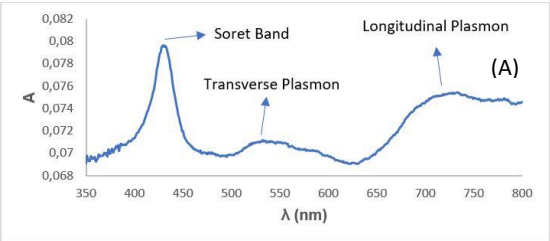

Figure 8 – UV-Vis absorption spectrum of hybrid system II (A) and III (B).

In both UV-Vis absorption spectra, it is possible to identify the Soret band (λ = 430 nm in (A) and λ = 428 nm in (B)) that is associated with the existence of TMPyP complexed with the PSS polyelectrolyte and a band around the value of 532 nm ((A)) and 522 nm ((B)) which corresponds to the transverse plasmon of the gold nanorods and another wide band centred at 720 nm which correspond to the longitudinal plasmon (Figure 8).

For Hybrid II, the values obtained for the number of moles adsorbed and adsorption efficiency were 1.32×10^{-11} mol and 0.576%, respectively. These values are too low because PSS adsorption promotes the porphyrin leaching. For Hybrid III, the values obtained for the number of moles adsorbed and adsorption efficiency were 1.81×10^{-9} mol and 78.8%. In this case, porphyrin is the most superficial layer of the hybrid so there is no reason for porphyrin to desorb.

Preparation of the system Hybrid IV:

By analyzing the UV-VIS absorption spectra of hybrid systems II and III, we can conclude that the adsorption of gold nanorods is accompanied by a shift of 50 nm from the longitudinal plasmon to the red zone of the electromagnetic spectrum. For porphyrin fluorescence enhancement to occur, there must be an overlap between the plasmon absorption spectrum and the porphyrin absorption and emission spectra, and the absorption and enhancement phenomena are maximum for the maximum plasmon wavelength [14]. In an attempt to obtain a system with spectral characteristics more suitable for observing the phenomenon of fluorescence enhancement by plasmonic effect, hybrid IV was prepared according to an experimental procedure similar to that previously described for hybrid II, but this time using gold nanoparticles with a longitudinal plasmon at λ = 614 nm.

Due to scattering it was not possible to obtain a typical UV-Vis spectra. However, there was a Shift from the longitudinal plasmon to λ = 762 nm, therefore, AuNR modification didn't result in the desired effect.

Fluorescence Enhancement by Plasmonic Effect

In this section, the influence of the architecture of the prepared systems on the enhancement of TMPyP fluorescence using gold nanorods as optical nanoantennas will be evaluated by fluorescence lifetime microscopy (FLIM), at λ_{exc} = 635 nm. Fluorescence intensity profiles were plotted across the individual capsule diameter and compared to those obtained for the control systems. At the same time, was carried out the timetrace of fluorescence bursts that may or may not result into a global intensification. Porphyrin fluorescence enhancement by plasmonic effect was based on the cherry-picking method. According to this method, the values of the enhancement factors ($\frac{F}{F_0}$) are calculated using equation (2):

$$\frac{F}{F_0} = \frac{I_e - I_{bg}}{I_{ne}} \qquad (2)$$

Where I_e corresponds to the highest fluorescence intensity value existing in a given fluorescence trace, I_{bg} corresponds to the value of the apparatus background counts I_{ne} symbolizes the fluorescence intensity value of the non-enhanced photosensitizer that, for the case of TMPyP is a constant value and equal to 0.8 cnts/s [19].

Despite of this analysis for all the systems, we will show the results for Hybrid II because in that system there is no photobleaching of the porphyrin and it was the architecture chosen for cytotoxic assays.

For control purposes, microcapsules containing only porphyrin ([PS]_PAHPSSPAHPSS_TMPyP_PSSPAH) or gold nanorods ([PS]_PAHPSSPAHPSS_[AuNR_PSS]) were also analyzed.

Fluorescence Enhancement by Plasmonic Effect – Hybrid II

An assessment of fluorescence intensity was made at various points on the microcapsules, in the control and hybrid systems.

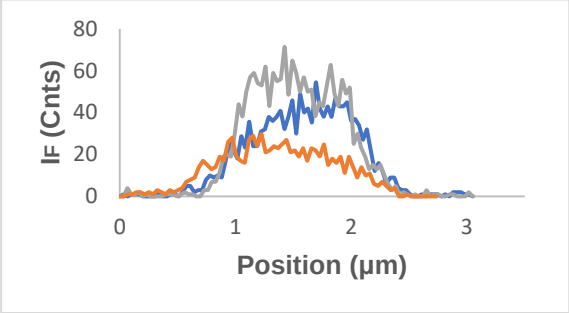

Figure 9 - Fluorescence Intensity Profile as a function of microcapsule position for the Hybrid II (—) and for the control systems with porphyrin (—) and with AuNR (—).

Fluorescence intensity of the hybrid system is similar to the fluorescence intensity that was obtained for the control system containing only the gold nanorods and slightly higher than the fluorescence intensity value obtained for the control system containing only porphyrin. As a result, plasmonic effect on global fluorescence enhancement is expected to be negligible.

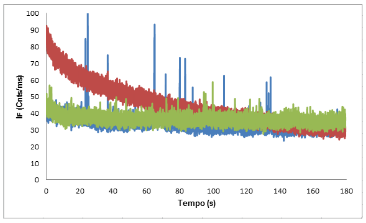

Figure 10 - Fluorescence intensity as a function of time for the systems: Hybrid II (—); Control with porphyrin (—) and Control with AuNR (—).

According to Figure 10, the measurement of the fluorescence traces for the two control systems is indicative of the absence of enhancement phenomena. Regarding the Hybrid II, it's possible to see some fluorescence enhancement events, whose values of $\frac{F}{F_0}$ are between 1.66×10^4 and 3.93×10^5. These values are lower than those reported in the literature[20] and it can be explained by the amount of TMPyP that is desorbed during PSS adsorption. Hence, the probability of a porphyrin molecule crossing a hot-spot located between two gold nanoparticles decreases and the occurrence of intensification phenomena is less frequent.

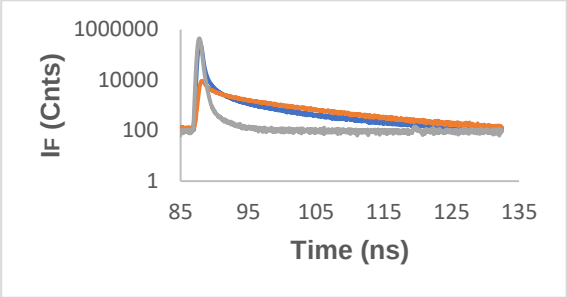

Figure 11 - Fluorescence Decay of Systems: Hybrid II, corresponding to one of the short duration events expressed in Figure 10 (—); Control with porphyrin (—) and Control with AuNR (—).

The Fluorescence decay of hybrid II can be represented by a tri-exponential function and subdivided into three distinct components: a very expressive short component, which is representative of the existence of gold nanoparticles on the surface of the microcapsules (≈0.3 ns), another that is around 8.8 ns and is associated with the complexation of TMPyP with PSS and a third component whose lifetime is equal to 1.5 ns [21].

To increase the occurrence of fluorescence enhancement phenomena, changes in the structure of the system were considered, namely, a second adsorption of TMPyP and an increase in the concentration of porphyrin in the adsorption solution.

Cytotoxicity Assays

Cytotoxicity assays were performed using HeLa cells originating from human adenocarcinoma, using resazurin as an indicator of cell viability for 24h, 48h and 72h of test. Resazurin is reduced to resorufin by the action of enzymes within cells. Resazurin has a λ_{max} absorption at 600 nm, whereas if it is converted to resorufin, there is a shift in the λ_{max} value to 570 nm [22]. Therefore, for each of the 3 days, after 4h of incubation after the addition of resazurin, the absorbance of the samples was measured at the wavelengths of 570 nm and 600 nm and he ratio between the mean absorbance values ($\frac{A_{570}}{A_{600}}$) was normalized.

In one of assays the plate with the compounds was irradiated with wavelength that corresponds to the red zone of the spectrum (P=17.59 mW/cm^2) to see if there is production of singlet oxygen in systems containing

porphyrin and what is the consequence in cell viability.

The structure of the systems studied were: Hybrid II.I – [PS]_PAHPSSPAHPSS_TMPyP_PAH_[AuNR-PSS]PAH; Hybrid II.II – [PS]_PAHPSSPAHPSS_TMPyP_PSS_TMPyP_PAH_[AuNR_PSS]; Controlo TMPyP – [PS]_PAHPSSPAHPSS_TMPyP_PAH and Controlo AuNR – [PS]_PAHPSSPAHPSSPAH_[AuNR-PSS]_PAH.

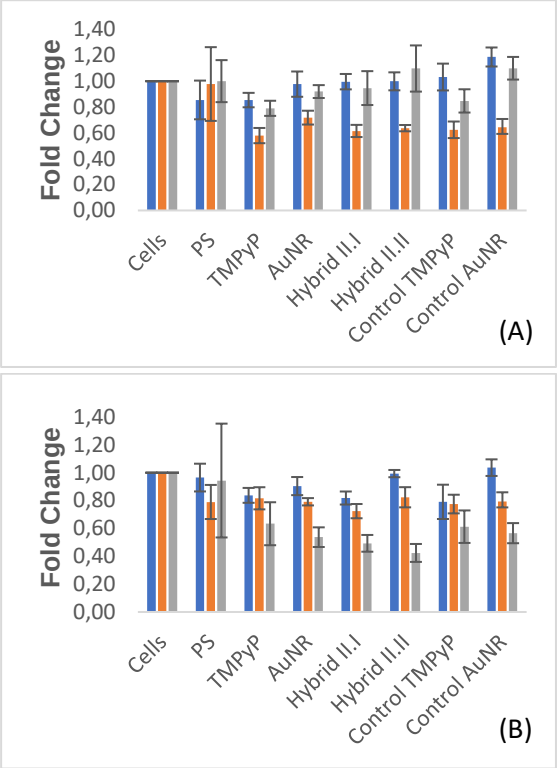

Figure 12 - Cytotoxicity tests using resazurin for non-irradiated (A) and irradiated (B) plates, for 24h (—), 48h (—) and 72h (—).

For the test in which there was no sample irradiation (Figure 12-A), after 24 hours it can be inferred that almost all resazurin was metabolized, with the exception of polystyrene microparticles and TMPyP.

In general, there is an increase in cell death from 24h to 48h. However, after 72h it is possible that the cytotoxic effect observed at 48h has stagnated and was overcome by the growth of cells that survived during the test and started their division process.

For the samples that were irradiated (Figure 12-B), porphyrin concentration used was about 0.024 μM to replicate the concentration of porphyrin existing in hybrid systems. In the systems containing porphyrin, there was an increase in cytotoxicity over time especially from 48h to 72h, which can be explained by the generation of singlet oxygen by TMPyP.

The decrease in cell viability after irradiation in wells containing AuNR and in the absence of TMPyP may be associated with a phenomenon of photothermal therapy. The radiation is absorbed by the gold nanorods and converted into heat, which promotes a local heating that may lead to cell death [23].

CONCLUSIONS AND FUTURE REMARKS

In this work, two different procedures were developed to obtain polyelectrolyte microcapsules. The two sets of microcapsules are distinguished from each other by the type of cores that served as the basis for the adsorption of polyelectrolyte molecules (polystyrene or $CaCO_3$).

In the polystyrene microcapsules the adsorption of the tetra-cationic porphyrin TMPyP and gold nanorods was carried out on the coating of the microcapsules. The spectroscopic properties were evaluated by UV-VIS absorption spectroscopy and fluorescence was studied by fluorescence lifetime microscopy (FLIM).

The relative position of these two components in the system was varied to promote the enhancement of porphyrin fluorescence through the action of the plasmonic antenna effect. The system Hybrid II was the one that presents the highest number of intensification events, without the photodegradation of the porphyrin. In the future, it is important to explore the concentration of porphyrin which promotes the fluorescence enhancement of the fluorophore, as well as the number of nanoparticles needed for an efficient coating of the microcapsules.

The study of the production of singlet oxygen in $CaCO_3$ capsules was analyzed through the degradation of DPBF, and the results were monitored by fluorescence emission spectroscopy and UV-VIS. It was concluded that the system with the porphyrin located in the most superficial part of the microcapsule produces an amount of singlet oxygen of at least 2.3 times greater than the other systems. As a future perspective, a study suggesting the production of singlet oxygen as a function of the concentration of porphyrin should be made.

Cytotoxicity assays were performed using HeLa cells originating from human adenocarcinoma, using resazurin as an indicator of cell viability. In one of the tests, the plate was not irradiated,

while in the other, radiation was focused on the plate with a wavelength in the red zone of the spectrum. In general, we can say that there is a greater loss of cell viability when the sample is irradiated, which is a result of the generation of singlet oxygen by TMPyP and the possible existence of a photothermal effect caused by the gold nanoparticles. In future work, it would be interesting to coat the microcapsules with other types of compounds (ex: folic acid, antibodies, etc.) to obtain better tumor cell uptake and internalization.

BIBLIOGRAPHY

[1] - Sung, H. *et al.*, Global Cancer Statistics 2020: GLOBOCAN Estimates of Incidence and Mortality Worldwide for 36 Cancers in 185 Countries. *CA: A Cancer Journal for Clinicians*, pp. 1-2, 2021.

[2] - Chinen, A. B *et al*., Nanoparticle Probes for the Detection of Cancer Biomarkers, Cells and Tissues by Fluorescence. *Chemichal Reviews*, vol. 115, pp. 10530-10539, 2015

[3] - Swain, S. M. Chemotherapy: Updates and New Perspectives, *The Oncologist*, vol. 16, pp. 30-39, 2011.

[4] - Alisson, R. R., Sibata, C. H. Oncologic photodynamic therapy photosensitizers: A clinical review. *Photodiagnosis and Photodynamic Therapy*, vol. 7, pp. 61-75, 2010.

[5] - Van Straten, D. *et al*., Oncologic Photodynamic Therapy: Basic Principles, Current Clinical Status and Future Directions. *Cancers*, vol. 9, pp. 1-54, 2017.

[6] - Agostinis, P. *et al*., Photodynamic Therapy of Cancer: An Update. *CA: A Cancer Journal for Clinicians*, vol. 61, pp. 250-281, 2011.

[7] - Aggarwal, A. *et al*., Porphyrinoid-based photosensitizers for diagnostic and therapeutic applications: An update. *Journal of Porphyrins and Phthalocyanines*, vol. 23, pp. 1-37, 2019.

[8] - Berg, K. *et al.*, Porphyrin-related photosensitizers for cancer imaging and therapeutic applications. *Journal of Microscopy*, vol. 218, pp. 133-147, 2005.

[9] - Francisco, A. P. *et al*., Extreme Enhancement of Single-Molecule Fluorescence from Porphyrins Induced by Gold Nanodimer Antennas. *The Journal of Physical Chemistry Letters*, vol. 10, pp. 1542-1549, 2019.

[10] - Huang, X., El-Sayed, M. A. Gold nanoparticles: Optical properties and implementations in cancer diagnosis and photothermal therapy, *Journal of Advanced Research*, vol. 1, pp. 13-28, 2010

[11] - Chen, H. *et al*., Gold nanorods and their plasmonic properties, *The Royal Society of Chemistry*, vol. 42, pp. 2679-2724, 2013.

[12] - Del Mercato, L. L. *et al*., Biological applications of LbL multilayer capsules: From drug delivery to sensing. *Advances in Colloid and Interface Science*. vol. 207, pp. 139-154, 2014.

[13] - Vergaro, V. *et al.*, Drug-loaded polyeletrolyte microcapsules for sustained targeting of cancer cells. *Advanced Drug Delivery Reviews*, vol. 63, pp. 847-864, 2011.

[14] - Munechika, K. *et al*., Spectral Controlo of Plasmonic Emission Enhancement from Quantum Dots near Single Silver Nanoprisms. *Nano Letters*, vol 10, pp. 2598-2603, 2010

[15] - Garcia-Sampedro, A. *et al*., Multimodal use of the porphyrin TMPyP: From cancer therapy to antimicrobial applications. *Journal of Porphyrins and Phathalocyanines*, vol. 23, pp. 1-17, 2019.

[16] - Sukhorukov, G. B. *et al*., Layer-by-layer self assembly of polyelectroytes on coloidal particles. *Colloids and* Surfaces. vol. 137, pp. 253-266, 1998.

[17] - Entradas, T. *et al*., The detection sensitivity of commonly used singlet oxygen probes in aqueous environments. Journal of Photochemistry & Photobiology, B: Biology, vol. 204, pp. 1-11.

[18] - Zhang, X. F., Li, X. The Photostability and fluorescence properties of diphenylisobenzofuran. *Journal of Luminescence*, vol. 131, pp. 2263-2266, 2011.

[19] - Francisco, A. P. *et al*., Extreme Enhancement of Single-Molecule Fluorescence from Porphyrins Induced by Gold Nanodimer Antennas. *The Journal of Physical Chemistry Letters*, vol. 10, pp. 1542-1549, 2019.

[20] - Petrov, A. I. *et al*., Base-Acid Equilibria in Polyelectrolyte Systems: From Weak Polyelectrolytes to Interpolyelectrolyte Complexes and Multilayered Polyelectrolyte Shells, *Macromolecules*, vol. 36, pp. 10079-10086, 2003.

[21] - Serra, V. V. *et al.*, Design of polyeletrolyte core-shells with DNA to control TMPyP binding. *Colloides and Surfaces B: Biointerfaces*, vol. 146, pp. 127-135, 2016.

[22] - Rezende, N. *et al.*, Standardization of a resazurina-based assay for the evaluation of metabolic activity in oral squamous carcinoma and glioblastoma cells. *Photodiagnosis and Photodynamic Therapy*, vol. 26, pp. 371-374, 2019.

[23] - Huang, X. *et al*., Cancer Cell Imaging and Photothermal Therapy in the Near-Infrared Region by Using Gold Nanorods. *American Chemical Society*, vol. 128, pp. 2115-2120, 2006.